PHYSICAL REVIEW E **77**, 040101(R) (2008)

Spontaneous symmetry breaking in amnestically induced persistence

Marco Antonio Alves da Silva,[1] G. M. Viswanathan,[2] A. S. Ferreira,[2] and J. C. Cressoni[2]
[1]*Departamento de Física e Química, FCFRP, Universidade de São Paulo, 14040-903 Ribeirão Preto, São Paulo, Brazil*
[2]*Instituto de Física, Universidade Federal de Alagoas, Maceió-AL, 57072-970, Brazil*

(Received 11 September 2007; revised manuscript received 28 January 2008; published 8 April 2008)

We investigate a recently proposed non-Markovian random walk model characterized by loss of memories of the recent past and amnestically induced persistence. We report numerical and analytical results showing the complete phase diagram, consisting of four phases, for this system: (i) classical nonpersistence, (ii) classical persistence, (iii) log-periodic nonpersistence, and (iv) log-periodic persistence driven by negative feedback. The first two phases possess continuous scale invariance symmetry, however, log-periodicity breaks this symmetry. Instead, log-periodic motion satisfies discrete scale invariance symmetry, with complex rather than real fractal dimensions. We find for log-periodic persistence evidence not only of statistical but also of geometric self-similarity.

DOI: 10.1103/PhysRevE.77.040101 PACS number(s): 05.40.Fb

I. INTRODUCTION

Exact solutions of non-Markovian processes appear infrequently and typically generate considerable interest (see, e.g., Ref. [1]), much more so when they involve non-Markovian systems that undergo one or more phase transitions. Here we investigate the symmetry properties and report the phase diagram for the recently reported phenomenon of amnestically induced persistence [2,3], which allows log-periodic [4] superdiffusion [5–7] driven by negative feedback. We show that a continuous scale invariance symmetry breaks down into a discrete symmetry. We also show that the critical line separating the log-periodic superdiffusive phase from the diffusive phase represents a distinct, smoother, phase transition. We report a total of four different phases for this non-Markovian system.

Random walkers without memory have a mean square displacement $\langle x^2 \rangle$ that scales with time t according to $\langle x^2 \rangle \sim t^{2H}$, with Hurst exponent $H=1/2$ as demanded by the central limit theorem, assuming finite moments. Hurst exponents $H>1/2$ indicate persistence and can arise due to long-range memory. Most random walks with and without memory display continuous scale invariance symmetry, i.e., continuous scale transformations by a "zoom" factor λ leave the Hurst exponent unchanged: $t^{2H} \rightarrow \lambda^{2H} t^{2H}$ as $t \rightarrow \lambda t$.

II. MODEL AND NUMERICAL RESULTS

Schütz and Trimper [1] pioneered a novel approach for studying walks with long-range memory [6–9], which we have adapted [2] for studying memory loss. Consider a random walker that starts at the origin at time $t_0=0$, with memory of the initial ft time steps of its complete history ($0 \leqslant f \leqslant 1$). At each time step the random walker moves either one step to the right or left. Let $v_t = \pm 1$ represent the "velocity" at time t, such that the position follows

$$x_{t+1} = x_t + v_{t+1}. \tag{1}$$

At time t, we randomly choose a previous time $1 \leqslant t' < ft$ with equal *a priori* probabilities. The walker then chooses the current step direction v_t based on the value of $v_{t'}$, using the following rule. With probability p the walker repeats the action taken at time t', and with probability $1-p$ the walker takes a step in the opposite direction $-v_{t'}$. Values $p>1/2$ ($p<1/2$) generate positive (negative) feedback. For p sufficiently larger than $p=1/2$, the behavior becomes persistent (i.e., $H>1/2$); but the finding of persistence for $p<1/2$ and small f overturned commonly held beliefs concerning repetitive behavior and memory loss [2]. Very recently, Kenkre [3] found an exact solution to this problem for the behavior of the first moment, for all f, and generalized it in important ways, with excellent agreement with the numerical results over six orders of magnitude in time. Here, we investigate how persistence depends quantitatively on memory loss and how to characterize the important underlying symmetry properties.

Figure 1(a) shows values of $H(f,p)$, estimated via simulations, as a function of the feedback parameter p and the memory fraction f. We choose an order parameter $2H-1$ that has positive values only in the persistent regime. Misleadingly, only two phases may at first seem apparent, namely, persistent and nonpersistent. However, we show further below, analytically, that each of these two regimes itself consists of two different phases with distinct symmetry properties, giving a total of four distinct phases.

For $p>1/2$ we find classical persistence satisfying continuous scale invariance symmetry. In contrast, we find discrete scale invariance symmetry [4] for $p<1/2$: scale invariance holds only for discrete values of the "zoom" or magnification $\lambda_k=\lambda^k$ ($k=1,2,3,\ldots$). The nonpersistent regime, similarly, comprises two phases: a classical diffusive phase and a log-periodic diffusive phase (see below). Mathematically, discrete scale invariance symmetry [4] involves complex fractal [11,12] dimensions: for $z=a+bi$, the real part of t^z equals $t^a \cos[b \log t]$, indicating log-periodicity [4]. Spontaneous symmetry breaking indicates a distinct phase (and eliminates the possibility of an infinite-order phase tran-

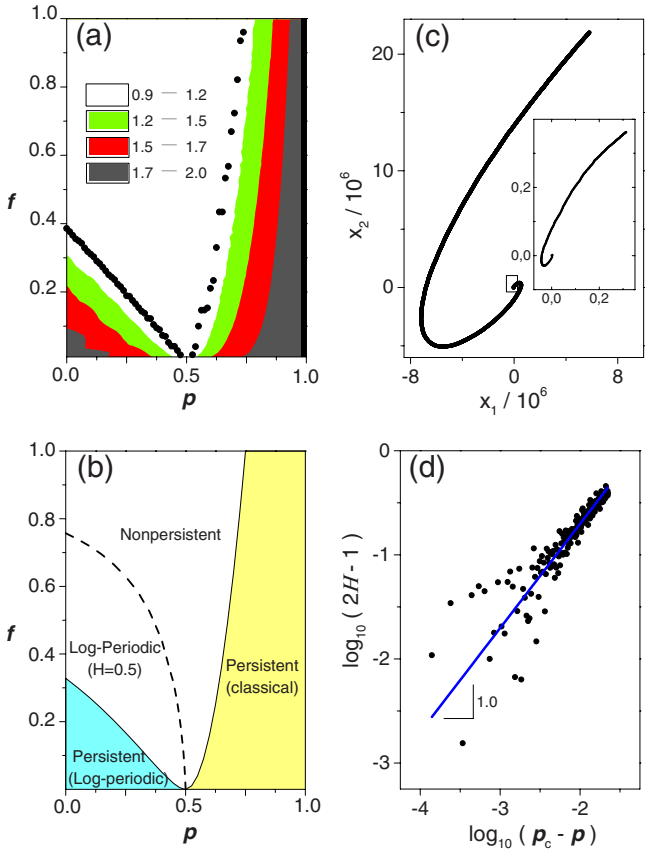

FIG. 1. (Color online) (a) Hurst exponent $H(p,f)$ estimated from simulations of non-Markovian walks that remember only a fraction f of their distant past, with feedback parameter p. Full circles show the edge where $H=1/2$. Persistence ($H>1/2$) arises for positive ($p>1/2$) as well as negative ($p<1/2$) feedback. (b) Complete phase diagram showing the four phases, plotted according to the exact solutions given by Eqs. (12) and (14). The dashed line $f_0(p)$ delineates the threshold for log-periodicity and cleaves the nonpersistent regime into two [Eq. (9)]. (c) Parametric plot of positions $x_1(t)$ and $x_2(t)$ for two realizations of log-periodic walks. Inset shows zoom of the center (boxed area) of the logarithmiclike spiral. Note the geometric self-similarity. (d) Double log plot of $2H-1$ versus p_c-p, showing critical behavior with critical exponent $\beta=1$.

sition) [10]. The simulation results agree well with our analytical results discussed further below [see Fig. 1(b)].

Figure 1(c) parametrically plots two independent persistent walks for $p<1/2$ ($p=0.1$ and $f=0.1$). The walks appear not only statistically but also geometrically self-similar. Indeed, we find a pattern reminiscent of a logarithmic spiral. We estimate a value of the critical exponent $\beta=1$ from the double log plot [Fig. 1(d)] of the order parameter versus $|p-p_c|$, where $p_c(f)$ denotes the critical line separating the diffusive and superdiffusive regimes.

III. ANALYTICAL RESULTS

We next approach the problem analytically. We choose $v_{t'}=\pm 1$ and use the previously discussed recurrence relation, Eq. (1). Let $n_f(t)$ and $n_b(t)$ denote the number of steps taken in the forward and backward directions, respectively, at time t (inclusive). The total number of steps equals $n_f(t)+n_b(t)=t$. For full memory, the probability to take a step in the forward direction at time $t+1$, for $t\geq 1$, is $P^+_{\text{eff}}(t)=\frac{n_f(t)}{t}p+\frac{n_b(t)}{t}(1-p)$. Similarly, $P^-_{\text{eff}}(t)=\frac{n_b(t)}{t}p+\frac{n_f(t)}{t}(1-p)$. So, the effective value expected at time $t+1$ equals $v^e_{t+1}=P^+_{\text{eff}}(t)-P^-_{\text{eff}}(t)$. Since $x_t=n_f(t)-n_b(t)+x_0$, we obtain $v^e_{t+1}=\alpha\frac{x_t-x_0}{t}$, where $\alpha=2p-1$. We can interpret this result as a series of experiments or walks at time t having the same number of steps forwards and backwards, giving the value v^e_{t+1}.

Now we introduce memory loss. Let the memory range be $L=L(t)=\text{int}(ft)$, where $\text{int}(x)$ denotes the integer part of x, for $0<f\leq 1$, starting at $t=0$. In analogy to the results above, we obtain $v^e_{t+1}=\alpha\frac{x_L-x_0}{L}$.

Now we study the nth moments of x^n_t. Taking Eq. (1) to power n we get $x^n_{t+1}=(x_t+v_{t+1})^n=\Sigma^n_{i=0}\binom{n}{i}v^i_{t+1}x^{n-i}_t$. For all even exponents i we know $v^i_{t+1}=1$ and for odd exponents $v^i_{t+1}=v_{t+1}$. Using the expression for v^e_{t+1}, with $x_0=0$, we obtain

$$\langle x^n_{t+1}\rangle=\Delta+\langle x^n_t\rangle+\frac{n\alpha}{L}\langle x_L x^{n-1}_t\rangle+\sum_{l=1}^{s(n)}\left[\binom{n}{2l}\langle x^{n-2l}_t\rangle+\frac{\alpha}{L}\binom{n}{2l+1}\langle x_L x^{n-2l-1}_t\rangle\right], \tag{2}$$

where $\Delta=\frac{1+(-1)^n}{2}$ and $s(n)=\frac{n-\Delta-1}{2}$. We have $\Delta=1$ for even n and $\Delta=0$ for odd n. If $s(n)<1$, then the sum vanishes.

In the asymptotic limit, we arrive at the following differential equation for the moments, starting from Eq. (2):

$$\frac{d}{dt}\langle x^n_t\rangle=\Delta+\frac{n\alpha}{L}\langle x_L x^{n-1}_t\rangle+\sum_{l=1}^{s(n)}\left[\binom{n}{2l}\langle x^{n-2l}_t\rangle+\frac{\alpha}{L}\binom{n}{2l+1}\times\langle x_L x^{n-2l-1}_t\rangle\right]. \tag{3}$$

For the first moment ($n=1$), we obtain an equation identical to the one obtained by Kenkre [3]:

$$\frac{d}{dt}\langle x_t\rangle=\frac{\alpha}{ft}\langle x_{ft}\rangle. \tag{4}$$

Considering an expansion of the form $\langle x_t\rangle\sim\Sigma_i A_i t^{\delta_i}\sin[B_i\ln(t)+C_i]$, we obtain a system of transcendental equations for B and δ:

$$\delta=\alpha f^{\delta-1}\cos(B\ln f) \tag{5}$$

$$B=\alpha f^{\delta-1}\sin(B\ln f). \tag{6}$$

For $\alpha\geq 0$, Eq. (5) leads to a maximum value of δ for $B=0$, which automatically satisfies Eq. (6). In any expansion, the term with the largest δ dominates, so $B=0$ should govern the long term behavior. We find no oscillations in our simulations, in agreement with this prediction. The two equations reduce to Eq. (7) below, ruling out a log-periodic solution. Note that for $p=1$, the ballistic solution forces $B=0$ exactly for any f. For $\delta>1/2$, we obtain superdiffusion (see below).

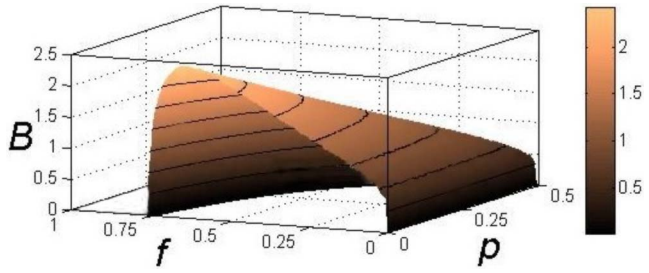

FIG. 2. (Color online) The angular log-frequency $B(f,p)$, estimated using Eq. (8), in the nonzero region. Interpreted as an order parameter, B quantifies a phase transition that breaks down continuous scale invariance symmetry ($B=0$) into a discrete symmetry ($B>0$).

For $\alpha<0$, there exists a threshold defined by a continuous set of values (p,f), with oscillating solutions. Consider first the case $B=0$, without oscillations. Then, Eq. (5) becomes

$$\delta = \alpha f^{\delta-1}, \tag{7}$$

which only has solutions for $f>f_0(p)$.

The appearance of log-periodicity breaks down continuous scale invariance symmetry into a discrete symmetry. We choose B as the order parameter for this phase transition, shown in Fig. 2. Equations (5) and (6) imply that the angular log-frequency B satisfies

$$B = \alpha f^{\{B/\tan[B\ \ln(f)]-1\}} \sin[B\ \ln(f)]. \tag{8}$$

Numerically solving Eq. (7), we find the threshold $f_0(0)=0.7569$ for $p=0$, in perfect agreement with the expression

$$(1-2p)\ln(1/f_0) = f_0/e, \tag{9}$$

obtained by Kenkre (personal communication, 13 July, 2007) for the onset of log-periodicity [3]. This critical line appears as a dashed line in Fig 1(b). We have found an alternative proof of Eq. (9) starting from Eq. (7), using the Lambert W function. For $\delta>1/2$, both superdiffusion and log-periodicity appear (see below).

We next study the second moment. If $n=2$ then $\Delta=1$ and $s(n)=0$. Thus Eq. (3) leads to

$$\frac{d}{dt}\langle x_t^2\rangle = 1 + \frac{2\alpha}{ft}\langle x_{ft}x_t\rangle. \tag{10}$$

Using the fact that $|\langle x\rangle| \leqslant (\langle x^2\rangle)^{1/2}$, we can prove that there exists a function $A(t)$ such that $\langle x_{ft}x_t\rangle = A(t)(\langle x_{ft}^2\rangle\langle x_t^2\rangle)^{1/2}$, with $-1\leqslant A(t)\leqslant 1$.

For $\alpha\geqslant 0$ ($p\geqslant 1/2$), no oscillations appear and $A(t\to\infty)=1$. We can thus show that the following transcendental relationship holds for the Hurst exponent, asymptotically:

$$H = \alpha f^{H-1}. \tag{11}$$

This result corresponds to Eq. (7) with $\delta=H$. Consequently, the curve

$$f_c = 16(p_c - 1/2)^2 \tag{12}$$

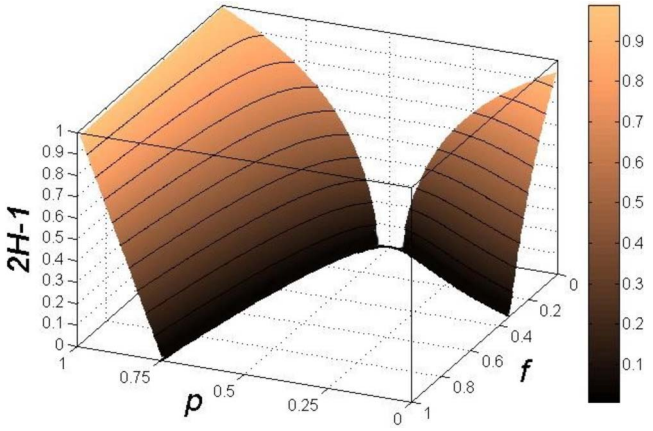

FIG. 3. (Color online) The order parameter $2H-1$ versus p and f in the nonzero (i.e., superdiffusive) region, estimated using Eqs. (11) and (13). Whereas B relates to the behavior of the first moment, H describes the second moment.

separates the diffusive and anomalous regions for $p\geqslant 1/2$ in the (p,f) plane [Fig. 1(b)]. The case $f=1$ leads to $p_c=3/4$, in agreement with Ref. [1].

For $\alpha<0$, we try the expansion $\langle x_t^2\rangle \sim \Sigma_i a_i t^{2H_i}\sin^2(b_i \ln t + c_i)$. We assume that the dominant terms of $\langle x_t\rangle$ and $\langle x_t^2\rangle$ have the same "period" and phase difference, so that $b=B$ and $c=C$. In the log-periodic region (i.e., $b\neq 0$), we also assume that $H\geqslant\delta$, so that the solution follows from Eqs. (5) and (6). Indeed we conjecture that for walks lacking subdiffusion, $\delta\geqslant 1/2$ implies $H=\delta$ always. The fact that $H>\delta$ for $\delta<1/2$ shows the importance of fluctuations and of higher moments [2] (and raises questions about possible multifractal scaling). Subject to natural restrictions, the Hurst exponent must thus satisfy

$$H\tan[\ln(f)\sqrt{\alpha^2 f^{2H-2} - H^2}] = \sqrt{\alpha^2 f^{2H-2} - H^2} \tag{13}$$

for $\delta\geqslant 1/2$ and $H=1/2$ otherwise. The separation line of the diffusive and anomalous phases [see Figs. 1(b) and 3] corresponds to the solution of Eq. (13) with $H=\delta=1/2$:

$$2\sqrt{\frac{\alpha_c^2}{f_c} - \frac{1}{4}} = \tan\left[\ln(f_c)\sqrt{\frac{\alpha_c^2}{f_c} - \frac{1}{4}}\right]. \tag{14}$$

We obtain the critical value of $f_c(0)=0.3284$ for the onset of log-periodic superdiffusion, which occurs at $p=0$. Note that $(p_c=1/2, f_c=0)$ represents a multicritical point.

The onset of superdiffusion thus represents a second, smoother, phase transition. Figure 3 shows a better view of how the order parameter $2H-1$ depends on p and f. The two phase transitions together yield a total of four different phases. Whereas B (Fig. 2) quantifies the behavior of the first moment, in contrast H (Fig. 3) relates to the second moment. Figure 1(a) numerically validates the complete phase diagram shown in Fig. 1(b).

Substituting our choice of $\langle x_t^2\rangle$ into Eq. (10), with the definition of $A(t)$, we obtain

$$A(t) = \frac{H \sin(b \ln t + c)^2 + b \sin(b \ln t + c)\cos(b \ln t + c)}{\alpha f^{H-1} |\sin(b \ln t + c)||\sin(b \ln ft + c)|}. \tag{15}$$

Semiempirically, we find that $A(t) \approx \pm 1$. Specifically, we propose

$$A(t) = \frac{\sin(b \ln t + c)\cos(b \ln ft + c)}{|\sin(b \ln t + c)\sin(b \ln ft + c)|}. \tag{16}$$

Note that $A(t)=1$ for $f=1$. Applying the same reasoning for the case $H=1/2$, we obtain

$$\begin{aligned} A(t) = f^{1/2}[2\alpha a|\sin(b \ln t + c)||\sin(b \ln ft + c)|]^{-1} \\ \times [a \sin(b \ln t + c)^2 + 2ab \sin(b \ln t + c) \\ \times \cos(b \ln t + c) - 1]. \end{aligned} \tag{17}$$

Thus, exactly on the critical line, we get a marginally superdiffusive solution: $\langle x^2(t)\rangle = at \ln t \sin^2(b \ln t + c)$. Numerical simulations suggest that higher order terms in the expansion become important near the critical line.

We next focus on finding a suitable Fokker-Planck equation (FPE). Let Y denote the position of a walker. Consider the conditional probability at position Y at time $t+1$, given position x_0 at time $t=0$:

$$\begin{aligned} P(Y,t+1|x_0,0) = P(Y+1,t|x_0,0)P^b_{\text{eff}}(t,Y+1) \\ + P(Y-1,t|x_0,0)P^f_{\text{eff}}(t,Y-1). \end{aligned} \tag{18}$$

Using the definitions of $n_f(t)$ and $n_b(t)$, and the probabilities to go forwards or backwards, we obtain

$$P^{\pm}_{\text{eff}}(t,Y) = (1/2)[1 \pm \alpha(Y - x_0)/t]. \tag{19}$$

Substituting Eq. (19) in Eq. (18), we get

$$\begin{aligned} P(Y,t+1|x_0,0) = (1/2)[1 - \alpha(Y - x_0 + 1)/t]P(Y+1,t|x_0,0) \\ + (1/2)[1 + \alpha(Y - x_0 - 1)/t]P(Y-1,t|x_0,0). \end{aligned} \tag{20}$$

From this last equation, in the asymptotic limit for t and Y, we get a FPE for $x=Y$, identical to the one in Ref. [1], as expected. The derivation of the FPE for $f<1$ proceeds in a similar manner (to be published in a future paper).

IV. CONCLUSION

In conclusion, we have uncovered the essential features of the phase diagram for this problem, based on numerical as well as analytical results. We expect the phase diagram and other findings reported here to contribute towards a better quantitative description of persistence in diverse economic [13], sociological [14], ecological [15], biological [5,15], and physiological [5] complex systems where recent memory loss may play a role [2]. We have found preliminary evidence of similarities between the log-periodic oscillations studied here with those found associated with financial bubbles [4]. In summary, an important result reported here relates to the atypical breaking of a continuous symmetry into a discrete one for a one-dimensional system. Another important result concerns the existence of a second phase transition which leads to a critical threshold of memory loss for the onset of superdiffusion.

ACKNOWLEDGMENTS

We thank V. M. Kenkre, M. L. Lyra, and the anonymous referees for comments. We thank CNPq and FAPESP (Grant No. 2007/04220-4) for funding.

[1] G. M. Schütz and S. Trimper, Phys. Rev. E **70**, 045101(R) (2004).
[2] J. C. Cressoni, Marco Antonio Alves da Silva, and G. M. Viswanathan, Phys. Rev. Lett. **98**, 070603 (2007).
[3] V. M. Kenkre, e-print arXiv:0708.0034v2 [cond-mat.stat-mech].
[4] D. Sornette, Proc. Natl. Acad. Sci. U.S.A. **99**, 2522 (2002).
[5] *Lévy Flights and Related Topics in Physics*, edited by M. F. Shlesinger, G. M. Zaslavsky, and U. Frisch (Springer, Berlin, 1995).
[6] R. Metzler and J. Klafter, Phys. Rep. **339**, 1 (2000).
[7] R. Metzler and J. Klafter, J. Phys. A **37**, R161 (2004).
[8] V. M. Kenkre, in *Statistical Mechanics and Statistical Methods in Theory and Application*, edited by U. Landman (Plenum, New York, 1977).
[9] V. M. Kenkre, E. W. Montroll, and M. F. Shlesinger, J. Stat. Phys. **9**, 45 (1973).
[10] H. E. Stanley, *Introduction to Phase Transitions and Critical Phenomena* (Oxford University Press, Oxford, 1971).
[11] B. B. Mandelbrot, *The Fractal Geometry of Nature* (Freeman, San Fransisco, 1982).
[12] A. Bunde and S. Havlin, *Fractals and Disordered Systems* (Springer, Berlin, 1991).
[13] R. N. Mantegna and H. E. Stanley, *An Introduction to Econophysics* (Cambridge University Press, Cambridge, England, 2000).
[14] B. J. West, *Mathematical Models As a Tool for the Social Sciences* (Taylor and Francis, London, 1980).
[15] P. Turchin, *Quantitative Analysis of Movements: Measuring and Modeling Population Redistribution in Animals and Plants* (Sinauer Associates, Sunderland, 1998).